WCTE 2018
2018 World Conference on Timber Engineering
August 20 - 23, 2018 | Seoul, Republic of Korea

# THE ROTATIONAL STIFFNESS OF CROSS-LAMINATED TIMBER HALF-LAP JOINTS

**Ewan Macpherson[1], Panayiotis Papastavrou[2], Tristan Wallwork[3], Simon Smith[4], Allan McRobie[5]**

**ABSTRACT:** Half-lap joints in cross-laminated timber are often conservatively assumed to have no rotational stiffness, preventing applications where the cross-joint stiffness could be utilised. The stiffness of a typical half-lap joint was derived from static four point bend tests, with experiments carried out through a combination of laboratory testing and finite element modelling. A simplified calculation method was developed to predict the rotational stiffness from the joint configuration and material properties. This was incorporated into a spreadsheet design tool for use by the industry partner.

**KEYWORDS:** Cross-laminated timber, Half-lap joint, Rotational stiffness, Particle Image Velocimetry, Finite element modelling

## 1 INTRODUCTION

A research project was undertaken at the University of Cambridge to investigate the rotational stiffness of half-lap joints. Half-lap joints are a common panel-to-panel connection in CLT, formed by cutting adjacent panels to half thickness and securing them with a line of self-tapping screws. The rotational behaviour of half-lap joints is poorly understood as they are typically only designed for normal and transverse forces [1]. However, joint stiffness influences serviceability criteria such as deflection or vibration which often govern the design of CLT structures. Quantifying and taking into account the rotational stiffness of half-lap joints could lead to applications in structures where cross-joint stiffness needs to be utilised.

## 2 MOTIVATION

The project was carried out collaboratively between academia and industry, with Smith and Wallwork Engineers commissioning the project and acting as advisers and sponsors. The inspiration for the project came from their design of a CLT folded plate roof for the Wynch Cottage building at Bishop's Stortford College seen in Figure 1.

***Figure 1:*** *Wynch Cottage interior ©Tim Crocker*

The roof consists of four triangular panels adjoining a pitched roof, with a shallow profile and a clear span of 12m. Due to transportation constraints, each triangular panel of the roof was made up of multiple CLT panels with half-lap joints between them. The complexity of the form and behaviour of folded plate roof structures means that their structural analysis is mainly based on the finite element method [2]. If cross-joint stiffness was known to contribute to the performance it could be incorporated into the model shown and lead to a more efficient design. The research project was commissioned to investigate the factors that contribute to half-lap joint rotational stiffness through a combination of finite element modelling and laboratory tests.

[1] Ewan Macpherson, Arup, Bristol, UK, ewan.macpherson@arup.com
[2] Panayiotis Papastavrou, Smith and Wallwork Engineers, Cambridge, UK, panayiotis@smithandwallwork.com
[3] Tristan Wallwork, Smith and Wallwork Engineers, Cambridge, UK, tristan.wallwork@smithandwallwork.com
[4] Simon Smith, Smith and Wallwork Engineers, Cambridge, UK, simon.smith@smithandwallwork.com
[5] Allan McRobie, Cambridge University Engineering Department, Cambridge, UK, fam@eng.cam.ac.uk

# 3 FINITE ELEMENT MODELLING

Finite element modelling of CLT panels with half-lap joints was carried out in Abaqus. Properties were assigned directly to individual CLT layers, making it possible to see the variation of stresses and deformation through the thickness of the panel. To model the half-lap joint in Abaqus, the interaction between the screw and timber must be successfully captured. The screw was modelled as a steel cylinder with a tie constraint to the surrounding timber to imitate the bonding action of the thread. At the timber to timber contact between the two half-lap pieces an interaction property was defined. The normal behaviour was set as a 'hard' contact whilst the tangential behaviour was assumed to be frictionless. A section through one of the models is shown in Figure 2.

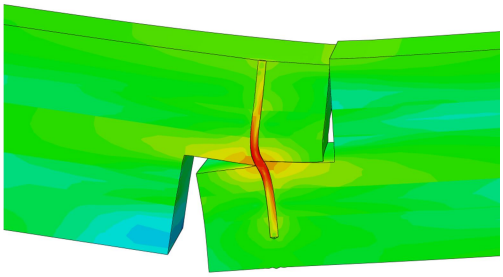

***Figure 2:*** *Section through Abaqus model of a four point bend test, showing principle stresses in the half-lap joint at mid-span*

# 4 ROTATIONAL STIFFNESS

## 4.1 LINEAR ROTATIONAL SPRING ANALOGY

A method was designed to determine the rotational stiffness from a simple load-deflection test. A four point bend test was chosen as it allows loads to be applied away from the joint and provides a constant moment through the central section. As the half-lap joint operates elastically under ordinary working loads, the joint can be assumed to act as a linear rotational spring. The deflection of the panel is formed of two components: the flexural and shear deflection from the panel itself and an additional deflection due to the rotation at the joint as illustrated in Figure 3.

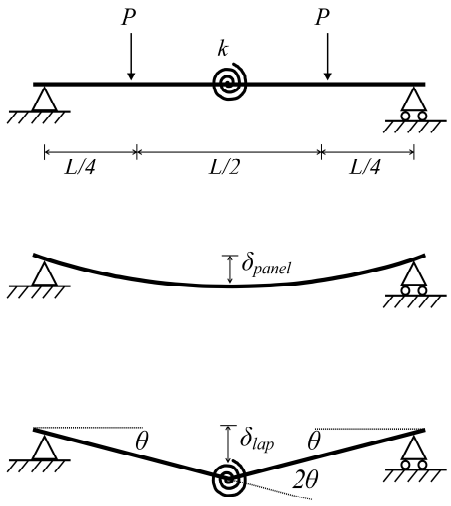


***Figure 3:*** *Rotational stiffness from mid-span deflection*

The rotational stiffness can be derived from the mid-span deflection by the principle of superposition:

$$\delta_{total} = \delta_{panel} + \delta_{lap} \quad (1)$$

$$M = \frac{PL}{4} = 2k\theta \quad (2)$$

$$\delta_{lap} = \frac{L}{2}\theta \quad (3)$$

$$k = \frac{PL^2}{16(\delta_{total} - \delta_{panel})} \quad (4)$$

# 5 SIMPLIFIED CALCULATION METHOD

## 5.1 FREE BODY DIAGRAM

A free body diagram through the half-lap joint reveals the shear and axial forces in the screw and the external forces at the corners applied by the adjacent panel. These combine to form two couples resisting the applied moment.

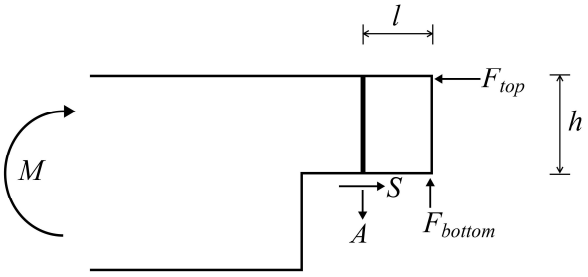


***Figure 4:*** *Free body diagram of half-lap joint*

For the joint to rotate there must be a point of contraflexure in the screw at mid-depth, so at the location of the cut the moment can be assumed to be negligible. To simplify the model, the normal forces at the timber contacts were represented by concentrated line loads and it was assumed that any friction forces could be neglected. As seen in Equations (5-7) there are three equilibrium equations and four unknown forces:

$F_{top} = S$ *(horizontal equilibrium)* (5)

$F_{bottom} = A$ *(vertical equilibrium)* (6)

$Sh + Al = M$ *(moment equilibrium about top right hand corner)* (7)

Therefore the problem has one degree of static indeterminacy which implies that a compatibility condition must be imposed to solve for the forces.

## 5.2 RIGID RECTANGLE MODEL

A number of processes occur to enable rotation of the half-lap joint, but it was postulated that local deformation in the screw and at the timber contacts would dominate any bending in the half-lap itself. On this basis a model was developed which assumes the region between the screw and the tip to act as a rigid rectangle, with four springs representing the stiffness

components as seen in Figure 5. The springs represent the combined effects of both halves of the joint, so a rotation of angle $2\theta$ is considered. The spring stiffnesses at the screw, $k_{shear}$ and $k_{axial}$, are therefore based on both halves of the screw while the timber spring stiffnesses, $k_{top}$ and $k_{bottom}$, correspond to the total compression of one piece relative to the other.

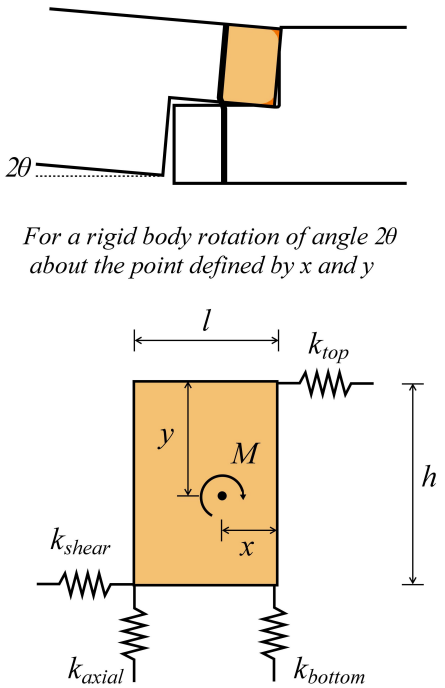


***Figure 5:*** *Rigid rectangle model*

The rotational stiffness of the joint can then be derived as a function of the spring stiffnesses in Equation (8).

$$M = \left( \frac{2h^2 \, k_{shear} \, k_{top}}{k_{shear} + k_{top}} + \frac{2l^2 \, k_{axial} \, k_{bottom}}{k_{axial} + k_{bottom}} \right) \theta \qquad (8)$$

## 5.3 SHEAR OF THE SCREW

The spring stiffness $k_{shear}$ represents the deformation of the embedded screw under a lateral load, a situation which can be modelled as a beam with bending stiffness $EI$ on an elastic foundation using the approach outlined by Hetenyi [3]. Assuming that the reaction provided by the foundation is proportional to its displacement $y$, as if it were a raft of springs of stiffness $\kappa$ per unit beam length, the fourth order beam bending equation becomes:

$$EI \frac{d^4 y}{dx^4} = -\kappa y \qquad (9)$$

This has a solution of the form:

$$y = e^{\lambda x}(C_1 \cos\lambda x + C_2 \sin\lambda x) + e^{-\lambda x}(C_3 \cos\lambda x + C_4 \sin\lambda x) \qquad (10)$$

$$\text{where } \lambda = \sqrt[4]{\frac{\kappa}{EI}} \qquad (11)$$

Extra complexity arises from the fact that the screw passes through several orthogonal CLT layers. Due to the anisotropic nature of the wood this changes the effective foundation modulus. The equations can be solved by imposing compatibility of displacement, rotation, moment and shear at each location where a transition between layers occurs. The boundary conditions for a two layer case are shown in Figure 6.

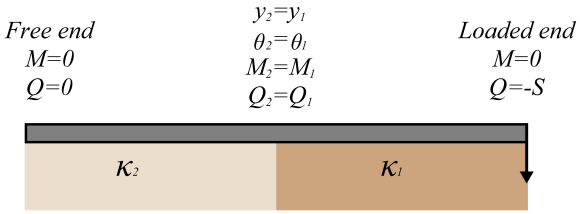


***Figure 6:*** *Beam on an elastic foundation analogy*

To generate solutions for any panel layup, the equations were converted to a matrix form which can be readily solved using Matlab. Comparison with Abaqus models allowed appropriate foundation moduli to be chosen for each layer direction within the CLT, shown in Table 1.

***Table 1:*** *Foundation moduli*

| Layer direction | κ (N/m$^2$) |
|---|---|
| Parallel to span | 9 x 10$^9$ |
| Perpendicular to span | 7 x 10$^8$ |

Figure 7 shows that changing the direction of the layers has a significant effect on the shear force diagram but the beam on an elastic foundation model was able to capture the majority of the behaviour.

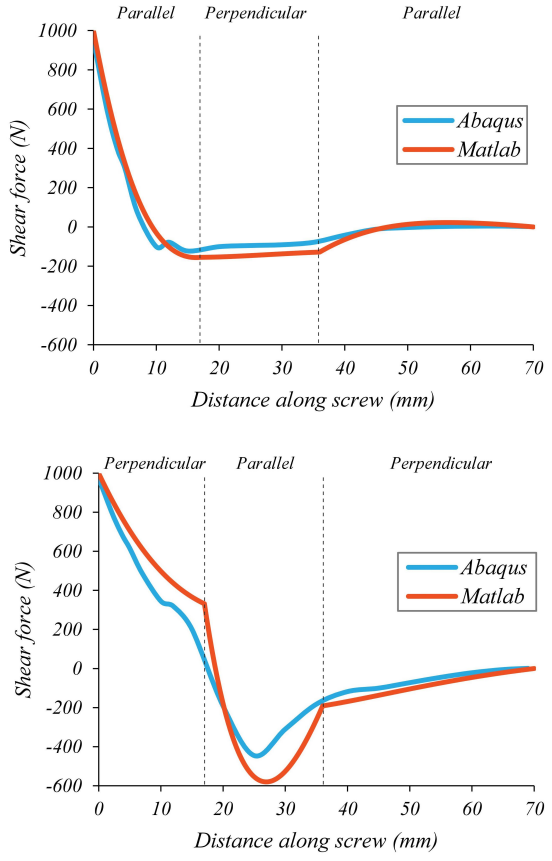


***Figure 7:*** *Shear force diagrams for an embedded screw (a) outer layers parallel, (b) outer layers perpendicular*

### 5.4 TENSION IN THE SCREW

To consider the stiffness of the axial spring, $k_{axial}$, an analogy was drawn between a screw in timber and a pile in soil. Each case considers the movement of a cylindrical element in a surrounding medium under axial load. The pile and soil are constrained to move together by friction at the interface; in the case of the screw the bond is provided by the thread.

The mode of deformation around a pile is primarily shear so the solution depends on the timber's shear modulus. This property is direction dependent with the rolling shear effect leading to a lower modulus in a plane perpendicular to the grain. As a first approximation for the analysis a constant shear modulus of 370 MPa was chosen, the mean of the moduli in each direction.

To take into account the relative stiffness of the screw and the timber, the analysis approach was based on Fleming's [4] solutions for a compressible pile. The displacement $\delta$ under an axial load $A$ is calculated as:

$$\frac{A}{\delta} = \frac{DG_{timber}\,\frac{2\pi}{\zeta}\,\frac{\tanh(\mu L)}{\mu L}\,\frac{L}{D}}{1+\frac{1}{\pi\lambda}\,\frac{8}{1-\nu}\,\frac{\tanh(\mu L)}{\mu L}\,\frac{L}{D}} \qquad (12)$$

$$\lambda = \frac{E_{screw}}{G_{timber}} \qquad \textit{(screw/timber stiffness ratio)} \qquad (13)$$

$$\zeta = \ln\left(5(1-\nu)\frac{L}{D}\right) \qquad \textit{(zone of influence)} \qquad (14)$$

$$\mu L = \frac{L}{D}\sqrt{\frac{8}{\zeta\lambda}} \qquad \textit{(screw compressibility)} \qquad (15)$$

where $D$ and $L$ are the screw diameter and embedment length respectively, $E_{screw}$ and $G_{timber}$ are the Young's and shear moduli of the screw and timber respectively and $\nu$ is the Poisson's ratio of the timber. To verify the analysis, the results were compared with simple Abaqus models of screw withdrawal encompassing several panel layups and embedment lengths. As seen in Figure 8 the pile model gives good agreement with the finite element results, capturing the magnitude of the displacements and general trend with embedment length.

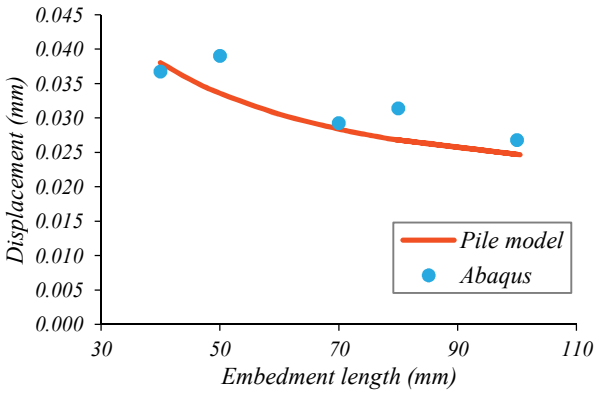


***Figure 8:*** *Comparison between pile analogy and finite element models for screw withdrawal*

### 5.5 COMPRESSION OF THE WOOD

The final two spring stiffnesses $k_{top}$ and $k_{bottom}$ are related to the compression of the timber at the half-lap corners. This can be visualised in Figure 9, which shows contours of contact pressure on an Abaqus model of one of the half-lap pieces.

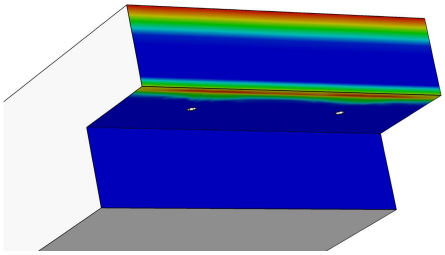

***Figure 9:*** *Abaqus image showing pressure at corner contacts*

As the behaviour of these regions is complex they do not lend themselves to a simple theoretical model; instead the stiffnesses were estimated and adjusted empirically by applying a known load to the corner regions in Abaqus and measuring the deflection. However, as the compression of the timber can be assumed to be primarily a local effect only two values of $k_{top}$ and $k_{bottom}$ are required depending on the direction of the timber in the corner region. The values used in the rigid rectangle model are shown in Table 2.

***Table 2****: Spring stiffnesses for timber compression, for a 200mm panel width*

| Spring | Direction | Stiffness (N/m) |
|---|---|---|
| $k_{top}$ | Outer layer parallel | $5.0 \times 10^6$ |
| | Outer layer perpendicular | $1.6 \times 10^6$ |
| $k_{bottom}$ | Middle layer parallel | $3.3 \times 10^6$ |
| | Middle layer perpendicular | $7.6 \times 10^5$ |

## 6 LABORATORY TESTS

Alongside the development of the theoretical model and Abaqus analysis, a range of physical experiments were carried out. The results were used to verify the assumptions that had been made throughout the project.

### 6.1 EXPERIMENTAL ARRANGEMENT

A testing rig was constructed to carry out four point bend tests in the laboratory, on continuous panels and panels with a half-lap joint at mid-span. Load was applied using a hydraulic jack via a spreader beam, whilst deflection was measured at mid-span using wire transducers as seen in Figure 10.

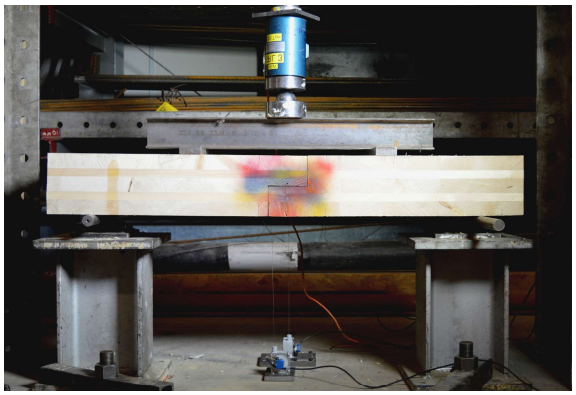

***Figure 10:*** *Laboratory testing rig*

### 6.2 PARTICLE IMAGE VELOCIMETRY

Particle Image Velocimetry (PIV) was used throughout the project as a visualisation technique. PIV uses a camera to track the movement of individual pixels and build up a displacement field for the area of interest in an experiment. This is particularly useful for tests in the elastic region as many of the movements are imperceptible to the naked eye but by using PIV the displacements can be animated and amplified.

### 6.3 CONTINUOUS PANEL TEST

To determine the rotational stiffness from the Abaqus models using Equation (4), the value of $\delta_{panel}$ was calculated using the Shear Analogy method [5]. The panel is modelled as two virtual beams coupled together. The first is assigned the stiffness of each layer about its own axis, while the second accounts for the parallel axis terms and shear stiffness of the panel. The Shear Analogy method is regarded as the most accurate method for predicting the stiffness properties of CLT panels [6]. The first laboratory experiment was designed to verify these calculations by comparing them with the deflections measured from Abaqus and a physical test. A series of three point bend tests were carried out on a three layer panel with a thickness of 80mm, the results are shown in Figure 11.

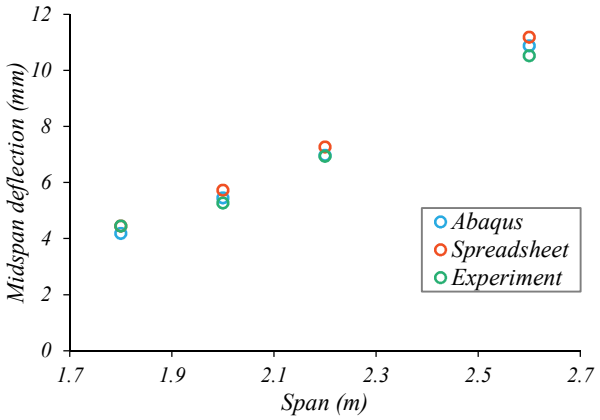


***Figure 11:*** *Comparison of deflections in continuous panels*

Excellent agreement was obtained between the three methods suggesting that the Shear Analogy calculations and Abaqus modelling techniques could be used reliably for continuous panels.

### 6.4 HALF-LAP JOINT ELASTIC TEST

The second experiment was a four point bend test using the same 80mm thick panel from the continuous panel test in Section 6.3, with the addition of a half-lap joint at mid-span. The panel was loaded at several different spans while the deflection was recorded.

By processing the results it was found that the rotational stiffness did not vary significantly with the span. This confirmed that the joint rotation could be isolated from the panel behaviour by the principle of superposition as outlined in Section 4.1.

The second conclusion from the experiment came from a PIV mesh defined over the region of the joint. A photograph was taken before and after loading. By subtracting the mean displacement of the region a PIV animation was used to display an amplification of the relative movement of pixels within the joint as shown in Figure 12.

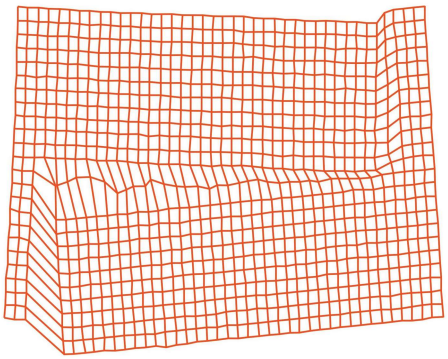

***Figure 12:*** *PIV animation showing amplified displacements during joint rotation*

This image clearly shows the rigid rectangle mechanism in action. Firstly the mesh lines within each piece remain straight throughout indicating that they are rotating relative to each other without significant deformation, authenticating the assumption of rigidity. Secondly, the timber compression can be identified as the mesh squares in the corners have distorted and decreased in size.

### 6.5 EXPOSED SCREW TEST

The final experiment was designed to observe the behaviour of a screw under load using PIV. Firstly, the screw was inserted close to the edge of the joint. Then the adjacent timber was gradually milled away until the screw could be seen but was still embedded securely as seen in Figure 13a.

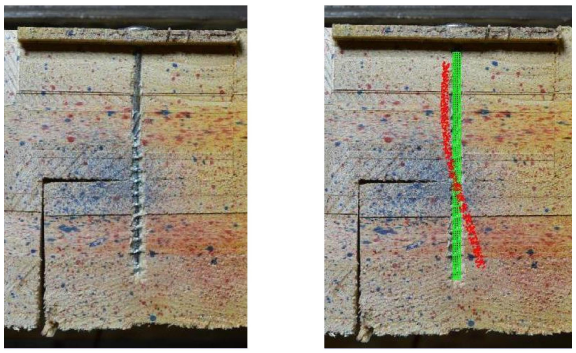

***Figure 13:*** *(a) An exposed screw within a half-lap joint (b) PIV image showing the displacement under load*

During the test it was not possible to identify any deformation of the screw with the naked eye. However, by defining a PIV mesh over the length of the screw (green in Figure 13b) the displacement could be plotted with a magnification factor (red in Figure 13b).
The screw's deflected shape shows a point of inflection at the joint boundary, indicating that the moment here is negligible as assumed in Section 5.1.

## 7 RESULTS

Using the spring stiffnesses derived in Sections 5.3 to 5.5, the rigid rectangle model was used to predict joint stiffness for sixteen different half-lap configurations. The results were compared with a series of Abaqus models; each panel had a width of 200mm and a single screw. The variables were selected to reflect common joint configurations within the CLT industry and the range of values used to construct the sixteen permutations are shown in Table 3.

***Table 3:*** *Half-lap joint configurations*

| | Layup | Direction | Lap length (mm) |
|---|---|---|---|
| 1 | 80 3 layer | Parallel | 90 |
| 2 | | | 50 |
| 3 | | Perpendicular | 90 |
| 4 | | | 50 |
| 5 | 140 5 layer | Parallel | 90 |
| 6 | | | 50 |
| 7 | | Perpendicular | 90 |
| 8 | | | 50 |
| 9 | 200 5 layer | Parallel | 90 |
| 10 | | | 50 |
| 11 | | Perpendicular | 90 |
| 12 | | | 50 |
| 13 | 201 7 layer | Parallel | 90 |
| 14 | | | 50 |
| 15 | | Perpendicular | 90 |
| 16 | | | 50 |

The results are shown in Figure 14, where the 45 degree line would indicate direct agreement between the two methods. There is close agreement for most configurations, showing that the rigid rectangle model is able to accurately represent and combine the underlying mechanisms that contribute to joint rotation.

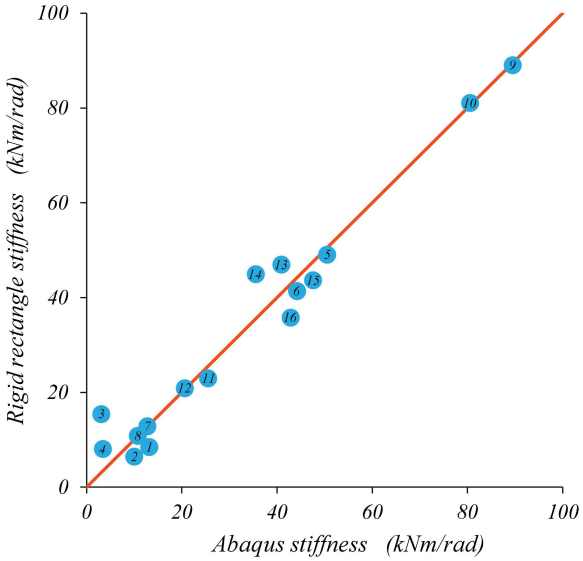


***Figure 14:*** *Rotational stiffness of half-lap joint from Abaqus and Rigid rectangle model, for a 200mm panel width*

It might be expected that increasing the lap length would lead to a significant increase in stiffness. However, as $h^2$ is much greater than $l^2$ for most common configurations the first term in Equation (8) dominates and the lap length has little impact. The panel thickness is therefore a more sensitive variable. This can be seen by comparing the results for panels 5-8 with 9-12. Each are 5 layer panels but increasing the thickness from 140mm to 200mm nearly doubles the stiffness.
The model also allows some counterintuitive results to be simply explained. For example, it seems surprising that panels 9 and 10 would be twice as stiff as panels 13 and 14 when the outer layers are spanning in the same direction and there is only a 1mm difference in thickness. However, this can be understood by considering the layup structure. In the 5 layer case the outer and middle layer are aligned so $k_{top}$ and $k_{shear}$ simultaneously take their maximum value. In the 7 layer case the middle layer is in the opposite orientation to the outer layer and the stiffness is greatly reduced.
The largest percentage errors are found in configurations 3 and 4, corresponding to the 80mm thick panel where the outer layer is perpendicular to the span. Figure 15 shows images from the finite element models for panels 1 and 3.

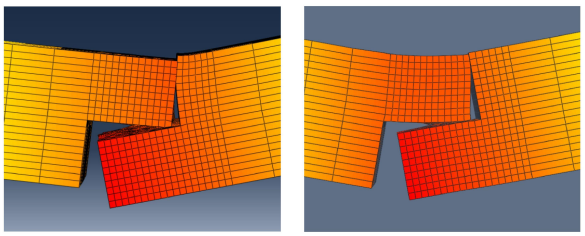

***Figure 15:*** *(a) Panel 1 - outer layer parallel to span (b) Panel 3 - outer layer perpendicular to span*

In the case of panel 3, it can be seen that the bending stiffness of the top half-lap piece is small enough that it deforms under load and the rigid rectangle assumption is

violated. However, panels of this depth are not commonly used so this is not a significant limitation of the model.

## 8 INITIAL IMPERFECTIONS

The Abaqus models represent idealised joints with a perfect fit but for the results to be applicable to industry they must take into account the condition of the joints as they appear in reality on a construction site. The cutting of joints takes place in a factory with a CNC machine under strictly controlled conditions, so there are minimal imperfections at the manufacturing stage. However, when the panels are placed and fixed on site there is often a gap of a few millimetres between adjacent panels, annotated as dimension *g* in Figure 16a.

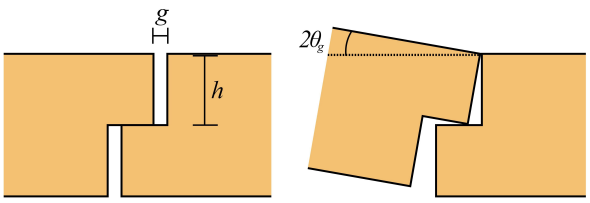


***Figure 16:*** *Half-lap joint with an initial imperfection (a) before rotation, (b) after rotation*

This situation can be easily described through the rigid rectangle model. Initially the force in the top timber spring is equal to zero as there is no contact, and by horizontal equilibrium the same must be true of the shear in the screw. The rotation is only resisted by the axial couple until the gap is closed:

$$M = \left(\frac{2l^2\, k_{axial}\, k_{bottom}}{k_{axial}+k_{bottom}}\right)\theta \qquad \text{For } 0 \le \theta < \theta_g \qquad (16)$$

$$\text{where } 2\theta_g = \frac{g}{h} \qquad (17)$$

Once the joint has rotated sufficiently for the gap to close it can be assumed the joint behaves as if it had an initially perfect fit. This method was verified against an Abaqus model. As predicted the results showed a bilinear moment rotation plot with an initial reduced stiffness equal to the resistance provided by the axial couple. As the half-lap joints are not designed to be moment resisting it is quite possible that gaps remain under working loads, therefore this reduced stiffness may be the more appropriate value for some applications.

## 9 CALCULATION SPREADSHEET

As a result of the research, a spreadsheet tool was developed for the industry partner to use in future projects. This is particularly valuable as many designers would not have access to 3D finite element software. The tool instantaneously predicts joint stiffness using the rigid rectangle model for a range of input variables, including a selection of over sixty panel layups from three prominent CLT manufacturers. It also includes an option to consider the effect of manufacturing imperfections by using the reduced stiffness discussed in Section 8.

## 10 CONCLUSIONS

CLT half-lap joints have a rotational stiffness, provided by two resisting couples comprising the internal forces in the screw and the compression at the corner timber contacts. This stiffness was quantified by considering a series of springs representing each stiffness component and imposing compatibility between them. In exploring theoretical models for screw shear and withdrawal, methods were developed which may have other applications within the field of timber connections.

A practical method was designed to measure joint stiffness in a four point bend test, allowing the results to be compared with Abaqus models. These 3D finite element models were found to be effective at investigating joint behaviour as they can capture the CLT's orthotropic properties as well as the interaction between the screw and surrounding timber. The theoretical model was able to accurately predict joint stiffness for a range of common configurations and also explained the sensitivity of joint stiffness to each variable.

Throughout the project, physical tests were used to inform and validate the assumptions in the theoretical model. PIV was used as a visualisation tool to understand the joint behaviour and would be a valuable method for many other applications in the field of structural testing, particularly for experiments focussed on small deformations in the elastic region.

The imperfections encountered in real structures were considered to ensure the findings are applicable to industry designers. Many designers also lack the time and resources to produce detailed computational models of joint behaviour. The research culminated in a simple spreadsheet based tool, allowing the industry partner to predict half-lap joint rotational stiffness quickly and effectively for many common joint configurations.

## REFERENCES

[1] Augustin, M.: Wood Based Panels. In Handbook 1. Timber Structures. TEMTIS, Ostrava, 2008.

[2] Marti, P.: Theory of Structures: Fundamentals, Framed Structures, Plates and Shells. Ernst and Sohn, Berlin, 2013.

[3] Hetenyi, M.: Beams on Elastic Foundation. University of Michigan Press, Michigan, 1946

[4] Fleming, K. *et al.*: Piling Engineering, Taylor & Francis, Abingdon, 2009

[5] Kreuzinger, H.: Platten, Scheiben und Schalen - Ein Berechnungsmodell für gängige Statikprogramme. *Bauen mit Holz,* 1:34-39, 1999

[6] FP Innovations: Cross-Laminated Timber Handbook, FP Innovations, Quebec, 2011